Supporting Information: The Quantified NTO Analysis for the Electronic Excitations of Molecular Many-Body Systems

Jian-Hao Li,[1,2] Jeng-Da Chai,[1,3] Guang-Yu Guo,[1,3,4] and Michitoshi Hayashi[2]

[1] *Department of Physics, Center for Theoretical Sciences, National Taiwan University, Taipei 10617, Taiwan*
[2] *Center for Condensed Matter Sciences, National Taiwan University, Taipei 10617, Taiwan*
[3] *Center for Quantum Science and Engineering, National Taiwan University, Taipei 10617, Taiwan*
[4] *Graduate Institute of Applied Physics, National Chengchi University, Taipei 11605, Taiwan*

(Dated: September 4, 2011)

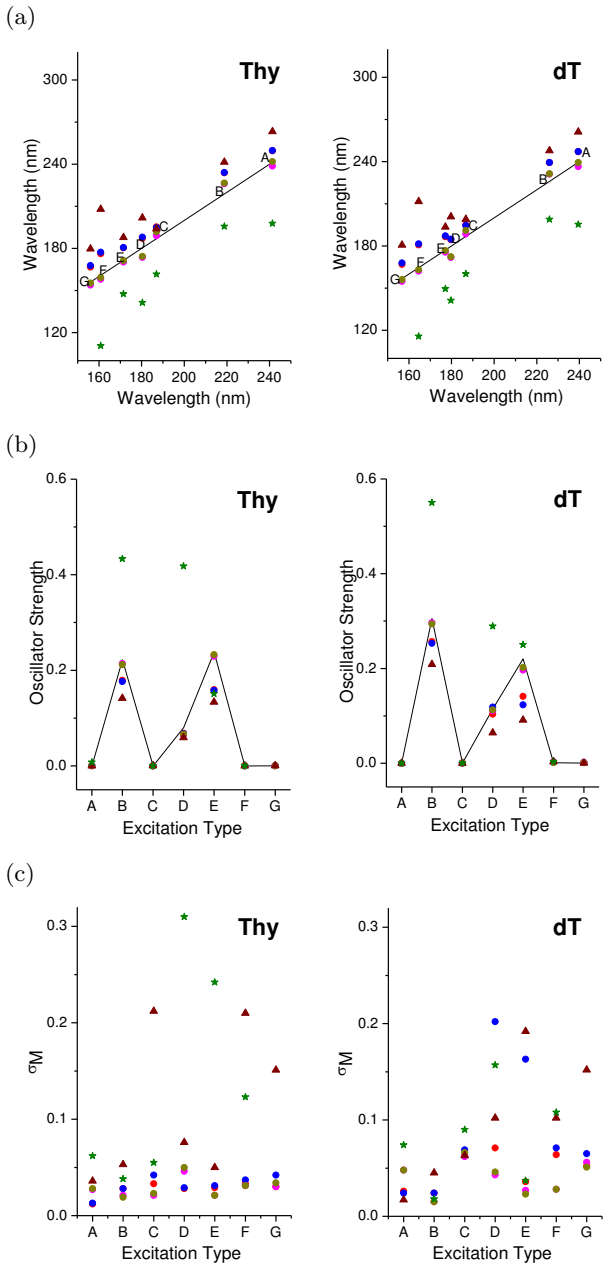

FIG. S1. The results of more theoretical methods not shown in Fig. 4. Notations are detailed in the main text. (a) Absorption wavelengths calculated using TD-CAM-B3LYP(●) [S1], TD-ωB97X-D(●) [S2], TD-ωB97(●) [S3], TD-LC-ωPBE(●) [S4] (LC hybrid functionals), TD-PBE1PBE(▲) [S5] (global hybrid functional) and CIS(⋆) [S6] (TD-HF with Tamm-Dancoff approximation) vs. absorption wavelengths from EOM-CCSD (／) [S7]. Data of each method for the same excitation lies on the same vertical line. (b) Oscillator Strength: line denotes the results from EOM-CCSD calculation. (c) σ_M of the Type-A∼Type-G excitations.

TABLE SI. Electronic transition origin of the first 8 SO-hosted singlet excitations of ideal Thy and dT given by calculation of (a) TDDFT with four different LC hybrid functionals: CAM-B3LYP, ωB97X-D, ωB97 and LC-ωPBE and (b) two other theoretical methods: CIS and TD-PBE1PBE not demonstrated in Table II. Incidentally, in CIS result of dT only 7 SO-hosted excitations out of the first 50 states (to 99.14nm for the 50th one) are recognized and listed. NTO1(2) stands for the (2nd) dominant natural transition orbital pair. P1, N1 and etc. are the standard-orbitals defined in Fig. 3 used to expand the hole- (NTO1(2)-H) and electron-orbital (NTO1(2)-E) of a NTO1(2). Subtitles N and P, respectively, denote the excitation order and the phase of NTO2 for the absorptions with NTO1 domination to the linear combination of singly excited configuration (LCSEC) lower than 70%. The next column shows the transition origin of NTO1(2), followed by the NTO1(2) domination to the excitation. The last column denotes the excitation classification based on EOM-CCSD Thy NTO1 expressions. The excitation denoted as (F') has similar Type-F NTO1 expression but larger σ_M.

(a)	Ideal Thy				Ideal dT			
	N; P	NTO1	%	Type	N; P	NTO1(2)	%	Type
TD-CAM-B3LYP	1	N1 - S1	100	A	1	N1 - S1	99	A
	2	P1 - S1	97	B	2	P1 - S1	97	B
	3	N1 N2 - (S1) S2	98	C	3	N1 N2 - (S1) S2	97	C
	4	P2 - S1	95	D	4	P1 - S2	69	E
	5	P1 - S2	94	E	-	P2 - S1	29	
	6	N2 - S1 (S2)	95	(F)	5	P2 - S1	71	D
	7	N1 N2 - S2	94	(G)	6	N2 B - S1 (S2)	92	(F)
	9	P2 - S2	93	-	7	N2 B - S1	91	(F')
					8	N1 N2 - S2	86	(G)
TD-ωB97X-D	1	N1 - S1	100	A	1	N1 - S1	99	A
	2	P1 - S1	96	B	2	P1 - S1	97	B
	3	N1 N2 - (S1) S2	97	C	3	N1 N2 - (S1) S2	96	C
	4	P2 - S1	94	D	4	P1 (P2) - (S1) S2	56	(E)
	5	P1 - S2	93	E	-	(P1) P2 - S1 (S2)	43	
	6	N2 - S1 (S2)	94	(F)	5	(P1) P2 - S1 (S2)	59	(D)
	7	N1 N2 - S2	94	(G)	+	P1 (P2) - (S1) S2	39	
	9	P2 - S2	94	-	6	N2 B - S1 (S2)	91	(F)
					7	N2 B - S1	89	(F')
					8	N1 N2 - S2	83	(G)
TD-ωB97	1	N1 - S1 (S2)	99	(A)	1	N1 - S1 (S2)	99	(A)
	2	P1 - S1	97	B	2	P1 - S1	97	B
	3	N1 N2 - S2	99	(C)	3	N1 N2 - S2	98	(C)
	4	P2 - S1	94	D	4	P1 - S2	90	E
	5	P1 - S2	93	E	5	P2 - S1	91	D
	6	N2 (O) - S1	94	(F)	6	N2 (B) (O) - S1	96	(F)
	7	N1 (N2) - (S1) S2	85	(G)	7	N1 (N2) - (S1) S2	81	(G)
	9	P2 - S2	94	-	8	(N2) B (O) - S1	80	(F')
TD-LC-ωPBE	1	N1 - S1 (S2)	100	(A)	1	N1 - S1 (S2)	99	(A)
	2	P1 - S1	97	B	2	P1 - S1	97	B
	3	(N1) N2 - S2	99	(C)	3	(N1) N2 - S2	99	(C)
	4	P2 - S1	94	D	4	P1 - S2	92	E
	5	P1 - S2	92	E	5	P2 - S1	93	D
	6	N2 (O) - S1	95	(F)	6	N2 (B) (O) - S1	97	(F)
	7	N1 (N2) - (S1) S2	85	(G)	7	N1 (N2) - (S1) S2	83	(G)
	8	P2 - S2	94	-	8	(N2) B (O) - S1	78	(F')

(b)	Ideal Thy				Ideal dT			
	N; P	NTO1(2)	%	Type	N; P	NTO1(2)	%	Type
CIS	1	N1 (N2) - S1 (S2) (O)	98	(A)	1	P1 - S1	94	B
	2	P1 - S1	94	B	2	N1 (N2) - S1 (S2) (O)	98	(A)
	3	(N1) N2 - S2 (O)	99	(C)	3	(N1) N2 - S2 (O)	97	(C)
	4	P1 P2 - S1 S2	59	(E)	4	P1 - S2	76	E
	+	P1 P2 - S1 S2	35		5	P2 - S1 (S2)	81	(D)
	6	P1 P2 - S1 S2	73	(D)	7	P2 - (S1) S2	87	-
	8	P2 - (S1) S2	88	-	15	(N1) N2 O - S1	45	(F)
	12	N1 N2 (O) - S1	64	(F')	-	P1 (B) - O	26	
	-	N1 N2 (O) - S2 (O)	32					
	15	N2 O - S1	68	(F)				
	+	N1 (N2) O - S2 (O)	23					
TD-PBE1-PBE	1	N1 - S1	100	A	1	N1 - S1	100	A
	2	P1 - S1	96	B	2	P1 - S1	97	B
	3	(N1) N2 - S1 (S2)	90	(F)	3	N2 B - S1	94	(F)
	4	P2 - S1	93	D	4	P2 - S1	80	D
	5	N1 N2 - (S1) S2	80	(C)	5	N1 (N2) - (S1) S2	61	(C)
	6	P1 - S2	90	E	-	B - S1 (S2)	37	
	7	(N1) N2 - S2	95	(G)	6	P1 (N1) (N2) - (S1) S2	69	(E)
	9	P2 - S2	90	-	+	(P1) (N2) P2 (B) - S1 (S2)	30	
					7	(P1) N2 (B) - S1 (S2)	64	(F)
					-	P1 (N1) B - (S1) S2	35	
					9	(N1) N2 - S2	92	(G)

RESULTS AND DISCUSSION

Importance of phase

While the phase between NTO1 and NTO2 leads to no difference for the physical properties associated with one-particle operators like electronic density,

$$\langle \Psi_i^a \pm \Psi_j^b | \hat{\rho}(\mathbf{r}) | \Psi_i^a \pm \Psi_j^b \rangle = \langle \Psi_i^a | \hat{\rho}(\mathbf{r}) | \Psi_i^a \rangle + \langle \Psi_j^b | \hat{\rho}(\mathbf{r}) | \Psi_j^b \rangle \quad (i \neq j)$$

, it is not for two-particle operators such as the interelectron coulomb repulsion.

On the other hand, in the case where i=j, the two SECs Ψ_i^a and Ψ_i^b become reducible when NTO transformation is performed, and the phase between them can make a difference even by a single-particle operator, e.g. $\hat{\rho}(\mathbf{r})$. It can be proved that $\langle \Psi_i^a + \Psi_i^b | \hat{\rho}(\mathbf{r}) | \Psi_i^a + \Psi_i^b \rangle \neq \langle \Psi_i^a - \Psi_i^b | \hat{\rho}(\mathbf{r}) | \Psi_i^a - \Psi_i^b \rangle$ because $\langle \Psi_i^a | \hat{a}_a^\dagger \hat{a}_b | \Psi_i^b \rangle$ connects the cross terms. For instance, this situation can be found on the TD-PBE1PBE result, where one finds that the NTO1 represented by "N1 N2 - (S1) S2" for the 5th excitation of Thy has a S1 phase difference compared to the NTO1, "N1 (N2) - (S1) S2", for the 5th excitation of dT.

Moreover, the relative phase between NTO1 and NTO2 can be absorbed into NTO1 or NTO2. For example, the complete expression for the 7th excitation of dT in the TD-PBE1PBE result reads $\sqrt{0.64}$"(P1) N2 (B) - S1 (S2)"-$\sqrt{0.35}$"P1 (N1) B - (S1) S2". Absorbing the relative phase between NTO1 and NTO2 into NTO2-H, for example, it can be rewritten as $\sqrt{0.64}$"(P1) N2 (B) - S1 (S2)"+$\sqrt{0.35}$"P1 (N1) B - (S1) S2" ('B' phase is not taken into account.)

Performance of various theoretical methods

Among the LC hybrid functionals used in Table SI(a), LC-ωPBE and ωB97 have the same HF-exchange operator (Fig. 5), while the others have different ones. LC-ωPBE and ωB97 give quite similar results for both Thy and dT, showing that the use of different versions of GGA in their functional forms matters little here and the fraction of HF-exchange with interelectron distance is much more important. We also see that CAM-B3LYP and ωB97X-D give quite similar results, which has also been found in [S8] for other molecular systems.

The coefficient threshold to output singlet excited configurations (SECs) for QNTO analysis in TDDFT calculations is set to 0.01; for EOM-CCSD it is set to 0.1 due to current software limitation. However, even though the threshold used is different, we assume the SECs with coefficient smaller than 0.1 have a minor effect on the composition of LCSEC so that EOM-CCSD results can be used as a good reference for TDDFT results for comparison.

Fig. 4, S1 and Table II, SI together show that TDDFT with LC hybrid functionals overall perform better than other methods for excitation energy, oscillator strength and NTO1 transition origin prediction. In general, CIS and TD-HF severely overestimate the excitation energy and oscillator strength, while TD-B3LYP, TD-PBE1PBE and TD-LDA underestimate them. The trend that pure density functional (LDA) and global hybrid functionals (B3LYP, PBE1PBE) tend to give a larger underestimation of oscillator strength for bright absorptions is also observed elsewhere of [S9]. The values of σ_M for different type of excitations yielded by the five methods are in most cases larger than those given by TDDFT with LC hybrid functionals. Moreover, LDA, having no HF-exchange in its functional form, leads to excitations with qualitatively different transition origins that generally cannot be well classified by Type-A∼Type-G. In fact if we focus on Type-B, D and E (bright absorptions), their relative absorption energy, oscillator strength, and NTO1 transition origin can be qualitatively captured by TD-B3LYP for both systems. However, for Type-C, F and G dark absorptions the description of NTO1 transition origin is more problematic and for Type-F its excitation energy is underestimated more significantly than other absorptions such that its order goes down; both properties play a significant role in later dynamics of an electronically excited molecule. TDDFT with LC hybrid functionals, on the other hand, can make them (and also excitation energy, oscillator strength) agree well with those predicted by EOM-CCSD.

We have observed a close relation between a proper description of electronic excitations and the prescription of HF-exchange in different functionals. LC hybrid functionals (LC-ωPBE, ωB97, ωB97X, ωB97X-D, CAM-B3LYP) are found to outperform global hybrid

functionals (B3LYP, PBE1PBE), pure density functional (LDA) and the exact-exchange (HF) method for excitation energy, oscillator strength and transition origin prediction, when compared with the EOM-CCSD results. It is also notable that the problematic description of Type-C, F and G excitations by B3LYP and PBE1PBE all concerns with N2-orbital involvement, which is HOMO-3, the deepest used standard-orbital from B3LYP KS-orbitals of Thy, and Type-C, G also concerns with S2-orbital, the LUMO+1, signifying that as (often higher-lying) electronic excitations are concerned with orbitals more far away from HOMO or LUMO, the correction of self-interaction error may be more important even if the system is as small as Thy.

[S1] T. Yanai, D. Tew, N. Handy, Chem. Phys. Lett. 393 (2004) 51.
[S2] J.-D. Chai, M. Head-Gordon, Phys. Chem. Chem. Phys. 10 (2008) 6615.
[S3] J.-D. Chai, M. Head-Gordon, J. Chem. Phys. 128 (2008) 084106.
[S4] O.A. Vydrov, J. Heyd, A.V. Krukau, G.E. Scuseria, J. Chem. Phys. 125 (2006) 074106.
[S5] C. Adamo, V. Barone, J. Chem. Phys. 110 (1999) 6158.
[S6] J.B. Foresman, M. Head-Gordon, J.A. Pople, M.J. Frisch, J. Phys. Chem. 96 (1992) 135.
[S7] R.J. Bartlett, M. Musial, Rev. Mod. Phys. 79 (2007) 291.
[S8] D. Jacquemin, E.A. Perpète, I. Ciofini, C. Adamo, Theor. Chem. Acc. 128 (2011) 127.
[S9] M. Caricato, G.W. Trucks, M.J. Frisch, K.B. Wiberg, J. Chem. Theory Comput. 7 (2011) 456.

Complete reference of Gaussian09

M. J. Frisch, G. W. Trucks, H. B. Schlegel, G. E. Scuseria, M. A. Robb, J. R. Cheeseman, G. Scalmani, V. Barone, B. Mennucci, G. A. Petersson, H. Nakatsuji, M. Caricato, X. Li, H. P. Hratchian, A. F. Izmaylov, J. Bloino, G. Zheng, J. L. Sonnenberg, M. Hada, M. Ehara, K. Toyota, R. Fukuda, J. Hasegawa, M. Ishida, T. Nakajima, Y. Honda, O. Kitao, H. Nakai, T. Vreven, J. A. Montgomery, Jr., J. E. Peralta, F. Ogliaro, M. Bearpark, J. J. Heyd, E. Brothers, K. N. Kudin, V. N. Staroverov, R. Kobayashi, J. Normand, K. Raghavachari, A. Rendell, J. C. Burant, S. S. Iyengar, J. Tomasi, M. Cossi, N. Rega, J. M. Millam, M. Klene, J. E. Knox, J. B. Cross, V. Bakken, C. Adamo, J. Jaramillo, R. Gomperts, R. E. Stratmann, O. Yazyev, A. J. Austin, R. Cammi, C. Pomelli, J. W. Ochterski, R. L. Martin, K. Morokuma, V. G. Zakrzewski, G. A. Voth, P. Salvador, J. J. Dannenberg, S. Dapprich, A. D. Daniels, O. Farkas, J. B. Foresman, J. V. Ortiz, J. Cioslowski, and D. J. Fox, Gaussian 09, Revision A.1, Gaussian, Inc., Wallingford CT, 2009.

TABLE SII. The standard-orbitals projection coefficients (coefficient square for orbital-fraction from backbone) of NTO1(2)-H(E) of several SO-hosted excitations calculated by (a) EOM-CCSD and TDDFT with LC hybrid functionals, and (b) several other theoretical methods shown in Table II and Table SI. λ(nm) and f column record absorption wavelengths and oscillator strengths, respectively. σ column records σ_E for EOM-CCSD and σ_M for other theoretical methods. In addition, there is data of the average σ shown in the method column.

(a)	Thy			NTO1(2)-H				NTO1(2)-E			dT			NTO1(2)-H					NTO1(2)-E		
	N	λ(nm)	f	P1	N1	P2	N2	S1	S2	σ	N	λ(nm)	f	P1	N1	P2	N2	$(B)^2$	S1	S2	σ
EOM-	1	241.40	0.0001	-0.01	0.96	-0.01	-0.23	0.94	0.28	-	1	239.47	0.0000	-0.02	0.96	-0.03	-0.22	0.01	0.95	0.20	0.024
CCSD	2	218.80	0.2220	0.99	0.01	0.01	0.00	0.99	-0.01	-	2	225.95	0.3051	0.98	0.02	0.02	0.00	0.02	0.98	0.00	0.006
(σ_E:	3	186.94	0.0000	-0.01	0.59	-0.01	0.80	-0.36	0.91	-	3	186.75	0.0004	-0.01	0.69	-0.05	0.66	0.05	-0.33	0.92	0.052
dT-0.029)	4	180.36	0.0802	-0.01	0.01	1.00	0.00	0.99	-0.01	-	4	179.74	0.1146	-0.02	0.04	1.00	0.02	0.00	0.98	0.00	0.012
	5	171.51	0.2382	1.00	0.01	0.01	0.00	0.01	0.99	-	5	177.08	0.2204	0.98	0.02	0.02	0.00	0.02	-0.01	0.97	0.011
	6	160.85	0.0001	0.00	0.27	-0.01	0.95	0.94	0.31	-	6	164.55	0.0009	0.03	0.21	-0.05	0.79	0.28	0.96	0.16	0.067
	8	156.00	0.0003	-0.01	0.83	0.00	-0.53	-0.27	0.92	-	7	156.79	0.0003	-0.02	0.84	-0.02	-0.48	0.04	-0.35	0.90	0.029
TD-	1	249.48	0.0002	-0.04	0.97	0.00	-0.25	0.94	0.27	0.012	1	247.05	0.0000	-0.01	0.96	0.00	-0.25	0.01	0.94	0.28	0.026
CAM-	2	233.87	0.1791	0.99	0.04	-0.08	0.00	1.00	-0.03	0.028	2	239.24	0.2568	0.98	0.01	-0.06	0.00	0.03	0.99	-0.02	0.024
B3LYP	3	195.27	0.0000	0.00	0.60	0.00	0.79	-0.46	0.86	0.033	3	194.94	0.0004	0.04	0.60	0.00	0.76	0.05	-0.47	0.85	0.063
(σ_M:	4	187.14	0.0683	0.08	0.00	1.00	0.00	1.00	-0.04	0.028	4	186.50	0.1413	0.97	-0.02	0.10	-0.03	0.03	-0.09	0.98	0.036
Thy-0.027;	5	180.42	0.1592	1.00	0.01	0.08	0.00	0.08	1.00	0.029				-0.10	-0.03	0.99	-0.01	0.01	0.98	0.08	
dT-0.048)	6	176.17	0.0000	0.00	0.28	0.00	0.95	0.91	0.42	0.033	5	184.44	0.1035	0.16	0.00	0.97	0.01	0.01	0.97	0.16	0.071
	7	166.72	0.0002	-0.01	0.78	0.00	-0.62	-0.28	0.94	0.030	6	180.74	0.0029	0.09	0.19	0.00	0.73	0.36	0.91	0.35	0.064
	9	155.18	0.3904	-0.08	0.00	0.99	0.00	-0.01	1.00	-	7	169.05	0.0067	-0.10	0.09	-0.03	0.61	0.53	0.98	-0.01	-
											8	166.90	0.0014	0.00	0.77	-0.01	-0.61	0.02	-0.26	0.94	0.052
TD-	1	249.72	0.0002	-0.04	0.97	0.00	-0.25	0.95	0.26	0.013	1	247.18	0.0000	-0.01	0.97	0.00	-0.25	0.00	0.94	0.27	0.024
ωB97X-D	2	234.05	0.1764	0.99	0.04	-0.08	0.00	1.00	-0.03	0.028	2	239.44	0.2531	0.98	0.01	-0.06	0.01	0.03	0.99	-0.02	0.024
(σ_M:	3	194.84	0.0000	-0.02	0.61	0.00	0.78	-0.49	0.85	0.042	3	194.60	0.0004	0.04	0.60	0.00	0.75	0.05	-0.50	0.84	0.069
Thy-0.032;	4	188.03	0.0673	0.08	0.00	0.99	0.00	1.00	-0.05	0.029	4	187.12	0.1232	0.89	-0.03	0.41	-0.03	0.03	-0.40	0.90	0.163
dT-0.088)	5	180.66	0.1580	0.99	0.01	0.09	0.00	0.08	1.00	0.031				-0.41	-0.01	0.91	0.01	0.01	0.90	0.39	
	6	177.27	0.0001	0.00	0.29	0.00	0.94	0.90	0.43	0.037	5	184.84	0.1186	0.46	-0.01	0.86	0.00	0.03	0.86	0.47	0.202
	7	167.82	0.0002	0.00	0.76	0.00	-0.65	-0.25	0.95	0.042				0.86	-0.02	-0.48	-0.02	0.02	-0.49	0.86	
	9	155.06	0.4063	-0.08	0.00	0.99	0.00	-0.02	1.00	-	6	181.44	0.0024	0.09	0.21	0.01	0.75	0.31	0.90	0.38	0.071
											7	169.70	0.0064	-0.10	0.05	-0.04	0.58	0.56	0.98	-0.06	-
											8	167.85	0.0018	0.00	0.75	-0.01	-0.64	0.02	-0.23	0.95	0.065
TD-	1	242.13	0.0002	-0.05	0.96	0.00	-0.28	0.92	0.31	0.021	1	239.80	0.0000	-0.01	0.96	0.00	-0.28	0.00	0.92	0.32	0.041
ωB97X	2	228.82	0.2013	1.00	0.05	-0.04	0.00	1.00	-0.05	0.022	2	233.96	0.2820	0.98	0.01	-0.02	0.00	0.03	0.99	-0.03	0.015
(σ_M:	3	190.78	0.0000	0.00	0.57	0.00	0.81	-0.35	0.90	0.009	3	190.28	0.0003	0.03	0.57	-0.01	0.79	0.03	-0.34	0.90	0.054
Thy-0.018;	4	178.49	0.0659	0.05	0.00	0.99	0.00	1.00	0.06	0.027	4	179.36	0.1967	0.98	-0.01	0.04	-0.02	0.03	0.04	0.98	0.019
dT-0.035)	5	174.43	0.1980	1.00	0.01	0.03	0.00	0.06	1.00	0.016	5	176.86	0.0825	0.02	-0.01	0.99	0.00	0.00	0.99	0.08	0.030
	6	164.14	0.0002	0.00	0.26	0.00	0.94	0.95	0.30	0.006	6	168.19	0.0015	0.05	0.20	0.00	0.74	0.29	0.95	0.24	0.032
	7	158.49	0.0003	-0.01	0.83	0.00	-0.55	-0.34	0.90	0.022	7	159.11	0.0010	0.00	0.78	0.02	-0.55	0.03	-0.48	0.84	0.051
	9	151.73	0.3700	-0.05	0.00	0.99	0.00	-0.08	1.00	-	8	156.42	0.0086	-0.08	0.28	-0.05	0.50	0.54	0.97	0.06	-
TD-	1	238.63	0.0002	-0.05	0.95	0.00	-0.29	0.91	0.33	0.027	1	236.44	0.0000	-0.01	0.95	0.00	-0.29	0.00	0.91	0.34	0.048
ωB97	2	226.03	0.2140	1.00	0.05	-0.02	0.00	1.00	-0.06	0.021	2	231.07	0.2966	0.98	0.02	-0.01	0.00	0.03	0.99	-0.04	0.015
(σ_M:	3	189.05	0.0000	0.00	0.55	0.00	0.83	-0.31	0.91	0.021	3	188.48	0.0002	0.03	0.55	-0.01	0.81	0.03	-0.31	0.91	0.062
Thy-0.028;	4	173.59	0.0642	0.08	0.00	0.99	0.00	0.99	0.12	0.046	4	175.51	0.1967	0.97	-0.01	0.05	-0.02	0.03	0.07	0.98	0.027
dT-0.040)	5	170.20	0.2295	1.00	0.01	-0.04	0.00	0.06	1.00	0.021	5	171.75	0.1108	-0.03	-0.01	0.99	0.00	0.00	0.98	0.14	0.043
	6	158.03	0.0004	0.00	0.24	0.00	0.91	0.97	0.22	0.031	6	162.13	0.0016	0.04	0.20	0.01	0.72	0.29	0.96	0.19	0.028
	7	153.85	0.0004	-0.01	0.85	0.00	-0.49	-0.36	0.89	0.030	7	154.77	0.0013	-0.01	0.79	0.02	-0.50	0.03	-0.51	0.81	0.056
	9	149.65	0.3419	-0.03	0.00	0.99	0.00	-0.14	0.99	-	8	150.79	0.0208	-0.05	0.30	-0.09	0.49	0.51	0.97	0.04	-
TD-	1	241.89	0.0002	-0.04	0.95	0.00	-0.29	0.91	0.34	0.028	1	239.42	0.0000	-0.01	0.95	0.00	-0.29	0.00	0.90	0.34	0.048
LC-ωPBE	2	226.50	0.2118	1.00	0.04	-0.02	0.00	1.00	-0.06	0.019	2	231.30	0.2938	0.98	0.02	-0.01	0.00	0.03	0.99	-0.04	0.015
(σ_M:	3	191.81	0.0000	0.00	0.54	0.00	0.83	-0.31	0.91	0.023	3	191.01	0.0002	0.03	0.54	-0.01	0.82	0.03	-0.30	0.91	0.066
Thy-0.029;	4	174.37	0.0663	0.09	0.00	0.99	0.00	0.99	0.13	0.050	4	176.69	0.2022	0.97	0.01	0.05	-0.02	0.03	0.06	0.98	0.023
dT-0.040)	5	171.41	0.2327	1.00	0.01	-0.04	0.00	0.06	1.00	0.021	5	172.37	0.1125	-0.02	-0.01	0.99	0.00	0.00	0.98	0.15	0.046
	6	159.28	0.0004	0.00	0.24	0.00	0.91	0.97	0.22	0.031	6	163.08	0.0014	0.04	0.20	0.01	0.72	0.28	0.96	0.19	0.028
	7	155.34	0.0004	-0.01	0.85	0.00	-0.49	-0.37	0.88	0.034	7	156.01	0.0010	-0.01	0.81	0.02	-0.49	0.03	-0.50	0.82	0.051
	8	150.72	0.3484	-0.03	0.00	0.99	0.00	-0.14	0.99	-	8	151.61	0.0317	-0.04	0.29	-0.12	0.49	0.51	0.97	0.03	-

(b)	Thy			NTO1(2)-H				NTO1(2)-E			dT			NTO1(2)-H					NTO1(2)-E		
	N	λ(nm)	f	P1	N1	P2	N2	S1	S2	σ	N	λ(nm)	f	P1	N1	P2	N2	$(B)^2$	S1	S2	σ
CIS	1	197.73	0.0077	-0.13	0.93	-0.01	-0.33	0.86	0.40	0.062	1	198.84	0.5502	0.98	0.01	0.03	0.00	0.02	0.98	-0.06	0.018
(σ_M:	2	195.68	0.4332	0.98	0.12	0.02	-0.04	0.99	-0.07	0.038	2	195.34	0.0001	-0.02	0.94	-0.01	-0.32	0.00	0.85	0.41	0.074
Thy-0.138;	3	161.65	0.0000	-0.01	0.47	-0.01	0.87	-0.23	0.91	0.055	3	160.17	0.0005	0.03	0.48	-0.02	0.86	0.02	0.23	-0.91	0.090
dT-0.080)	4	147.53	0.1508	0.80	0.02	0.58	0.00	0.56	0.80	0.242	4	149.55	0.2503	0.98	0.00	0.07	-0.03	0.03	-0.10	-0.98	0.037
				-0.59	0.00	0.79	0.00	0.79	-0.58		5	141.28	0.2894	-0.21	0.00	0.96	0.01	0.00	0.85	0.49	0.157
	6	141.31	0.4179	-0.61	0.00	0.78	0.01	0.62	0.77	0.310	7	126.31	0.2175	0.10	0.03	0.97	-0.01	0.00	0.41	-0.90	-
	8	126.65	0.2298	0.13	0.01	0.97	0.00	-0.38	0.92	-	15	115.65	0.0033	0.04	-0.46	0.01	-0.56	0.07	0.96	0.03	0.108
	12	116.52	0.0004	0.00	0.59	-0.01	0.61	0.98	0.01	-				0.90	0.09	0.14	0.02	0.13	-0.08	0.05	
				-0.01	0.63	0.00	-0.66	0.05	0.93												
	15	110.63	0.0001	0.00	0.03	0.00	0.63	0.98	0.17	0.123											
				-0.02	0.69	0.00	-0.40	-0.19	0.92												
TD-HF	1	206.52	0.3427	0.98	-0.04	0.04	0.02	0.99	-0.07	0.025	1	209.49	0.4576	0.97	0.01	0.04	0.00	0.01	0.98	-0.06	0.019
(σ_M:	2	202.72	0.0021	0.05	0.94	0.00	-0.33	0.85	0.41	0.057	2	200.20	0.0000	-0.02	0.94	-0.01	-0.32	0.00	0.84	0.41	0.075
Thy-0.137;	3	164.91	0.0000	-0.01	0.47	-0.01	0.87	-0.23	0.91	0.055	3	163.31	0.0005	0.04	0.48	-0.02	0.86	0.02	0.23	-0.91	0.090
dT-0.106)	4	152.36	0.1127	0.65	0.01	0.73	0.00	0.70	0.67	0.297	4	153.99	0.1954	0.97	0.00	0.09	-0.04	0.02	-0.11	-0.97	0.042
				-0.75	-0.01	0.64	0.00	0.67	-0.73		5	144.95	0.2422	-0.31	0.01	0.93	0.02	0.00	0.79	0.59	0.199
	5	144.72	0.3622	0.66	0.00	-0.74	0.00	0.53	0.84	0.284	7	128.95	0.1427	0.14	0.04	0.96	-0.01	0.00	0.43	-0.89	-
	8	129.32	0.1426	0.18	0.03	0.95	-0.01	-0.41	0.90	-	15	116.43	0.0077	0.50	-0.30	0.07	-0.39	0.28	0.69	0.06	0.211
	15	111.24	0.0004	0.00	0.08	0.00	0.65	0.97	0.21	0.107				0.70	0.32	0.08	0.34	0.04	0.64	-0.02	
	22	100.71	0.0099	0.61	0.06	0.05	0.00	-0.13	0.70	-	21	110.25	0.0317	0.96	0.03	0.01	0.00	0.02	0.87	0.25	-
				-0.02	0.88	-0.01	0.44	0.01	-0.04												
TD-	1	270.56	0.0001	-0.04	0.99	0.00	-0.15	0.99	0.15	0.048	1	268.35	0.0001	-0.03	0.98	0.00	-0.15	0.01	0.97	0.16	0.026
B3LYP	2	246.47	0.1268	0.97	0.04	-0.21	0.00	1.00	0.00	0.064	2	253.13	0.1897	0.94	0.02	-0.16	-0.03	0.07	0.99	0.01	0.054
(σ_M:	3	216.14	0.0000	0.00	0.25	0.00	0.96	0.97	-0.24	0.159	3	220.32	0.0042	0.15	0.11	-0.02	0.74	0.37	0.98	-0.10	0.089
Thy-0.116;	4	208.21	0.0574	0.23	0.00	0.97	0.00	0.97	-0.22	0.093	4	207.29	0.0591	0.26	-0.03	0.96	-0.04	0.01	0.95	-0.28	0.118
dT-0.110)	5	200.48	0.0001	-0.05	0.91	0.00	0.40	0.10	0.99	0.200	5	205.43	0.0003	-0.16	0.53	0.12	0.53	0.39	-0.87	0.47	0.221
	6	192.17	0.1223	0.99	0.04	0.15	0.05	0.14	0.99	0.058				0.01	0.69	-0.15	0.12	0.45	0.46	0.86	
	7	184.80	0.0002	0.03	0.38	0.00	-0.92	-0.03	1.00	0.187	6	200.39	0.0014	0.08	0.67	0.11	0.68	0.07	0.60	0.77	-
	9	162.81	0.3352	-0.16	0.00	0.98	0.00	0.01	1.00	-				0.21	0.62	-0.07	-0.43	0.35	-0.78	0.61	
											7	197.43	0.1530	0.96	-0.04	0.18	-0.04	0.04	0.19	0.95	0.077
											9	186.15	0.0003	-0.04	0.42	0.00	-0.87	0.06	-0.07	0.98	0.186
TD-	1	263.26	0.0001	-0.04	0.98	0.00	-0.18	0.98	0.18	0.036	1	261.13	0.0001	-0.03	0.98	0.00	-0.18	0.01	0.97	0.19	0.017
PBE1PBE	2	241.45	0.1414	0.98	0.04	-0.17	0.00	1.00	-0.01	0.053	2	247.82	0.2086	0.95	0.02	-0.13	-0.02	0.06	0.99	0.00	0.045
(σ_M:	3	207.93	0.0000	-0.01	0.37	0.00	0.92	0.91	-0.41	0.210	3	211.64	0.0033	0.13	0.17	-0.01	0.74	0.37	0.97	-0.17	0.102
Thy-0.113;	4	201.76	0.0589	0.19	0.00	0.98	0.00	0.98	-0.18	0.076	4	200.76	0.0643	0.22	-0.03	0.97	-0.03	0.01	0.96	-0.24	0.102
dT-0.096)	5	193.99	0.0002	-0.05	0.79	0.00	0.61	0.32	0.95	0.212	5	199.04	0.0001	-0.11	0.82	0.02	0.54	0.03	-0.37	0.92	0.063
	6	187.83	0.1333	0.99	0.04	0.13	0.05	0.12	0.99	0.050				-0.10	-0.13	0.19	0.02	0.89	0.91	0.35	
	7	179.67	0.0002	0.02	0.49	0.00	-0.87	-0.08	1.00	0.151	6	193.41	0.0911	0.79	0.38	0.23	0.35	0.05	0.32	0.92	0.192
	9	159.34	0.4077	-0.13	0.00	0.99	0.00	0.02	1.00	-				-0.40	-0.17	0.61	0.52	0.14	0.93	-0.33	
											7	192.11	0.0688	-0.41	0.29	-0.28	0.69	0.20	0.87	0.45	-
														0.63	-0.47	-0.15	0.17	0.31	-0.46	0.87	
											9	180.60	0.0003	-0.02	0.53	0.01	-0.82	0.04	-0.11	0.98	0.152
TD-	1	316.41	0.0000	-0.03	1.00	0.00	0.05	1.00	-0.04	0.125	1	316.27	0.0006	-0.07	0.95	0.02	0.07	0.07	0.99	-0.02	-
LDA	2	270.51	0.0662	0.90	0.03	-0.40	0.05	0.99	0.08	0.125	2	291.65	0.0413	0.50	0.27	-0.16	-0.28	0.53	0.99	0.01	-
(σ_M :	3	267.18	0.0003	-0.05	-0.05	0.01	0.99	1.00	-0.01	0.133	3	271.79	0.0622	0.67	-0.08	-0.25	0.59	0.11	0.98	0.05	-
Thy-0.201)	4	236.19	0.0011	-0.08	0.99	-0.03	-0.07	0.04	1.00	0.170	5	254.91	0.0125	-0.33	0.07	0.14	0.73	0.34	0.99	0.03	-
	5	235.14	0.0507	0.43	0.06	0.90	0.01	0.91	-0.40	0.174	6	239.34	0.0006	-0.08	0.97	-0.02	-0.05	0.04	0.01	0.98	-
	6	208.80	0.0944	0.97	0.04	0.20	0.02	0.22	0.97	0.083	7	235.80	0.0456	0.40	0.05	0.86	-0.03	0.09	0.90	-0.41	-
	7	203.29	0.0001	-0.02	0.06	-0.01	0.99	0.00	1.00	0.195	9	220.59	0.0679	0.42	0.15	0.03	-0.33	0.65	0.02	0.97	-
	11	173.87	0.2857	-0.19	0.00	0.97	0.01	-0.05	1.00	-	10	214.82	0.0548	0.78	-0.05	0.15	0.35	0.22	0.11	0.93	-
				0.34	-0.01	0.16	0.00	1.00	0.05												